Journal of Applied Chemistry

JAC
http://chemistry.journals.semnan.ac.ir

Nanoparticles of SBA-15 synthesized from corn silica as an effective delivery /system for valproic acid

Faeze Khanmohammadi[1,2], Bibi Marziyeh Razavizadeh[2], Seyed Naser Azizi [1,*]

[1]*Analytical Division, Faculty of Chemistry, University of Mazandaran, Babolsar, Iran*

[2]*Department of Food Safety and Quality Control, Research Institute of Food Science and Technology, Mashhad, Iran*

Article history:
Received:22/ May /2022
Received in revised form: 14/July/2022
Accepted: 08/Aug/2022

Graphical abstract

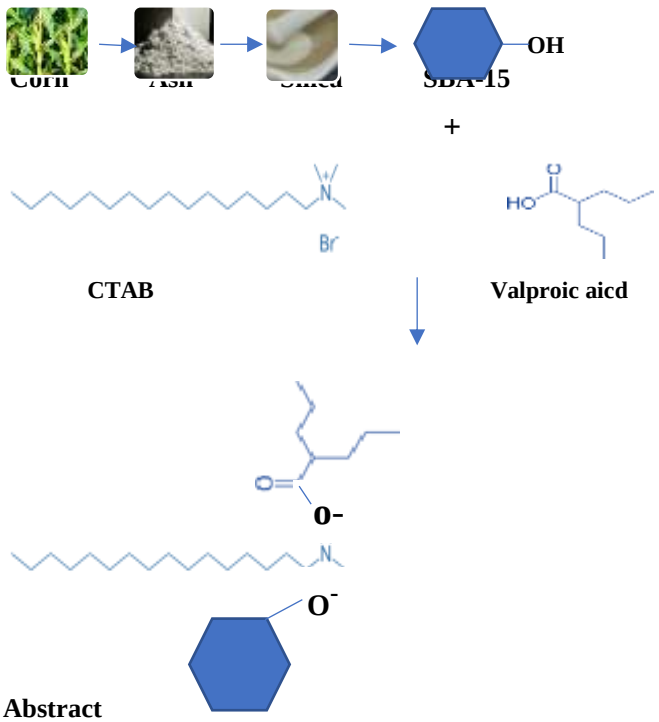

Abstract

The aim of this work is to study the behavior of SBA-15 synthesized using amorphous silica extracted from different parts of the corn plant, as drug carriers. The synthesized nano-silica and mesoporous SBA-15 were characterized by x-ray diffraction (XRD), thermogravimetric analysis (TGA), x-ray fluorescence (XRF), scanning electron microscopy (SEM), transition electron microscopy (TEM), Fourier transform infrared (FT-IR), and N_2 isotherms. SEM and TEM images showed that SBA-15 is formed by spongy agglomerated nanoparticles revealing the growth of hexagonal shaped domains. The synthesized SBA-15 was modified with cetyltrimethylammonium bromide (CTAB), to increase the carriers' capacity. The SBA-15 and modified SBA-15 show hexagonal order with decreasing pore size from 7.5 nm to 5.5 nm after modification, and surface area from 488 m^2/g to 127.75

* **.Corresponding author:** Professor of Analytical Chemistry, Mazandaran University, Babolsar, Iran. *E-mail address: seyednaserazizi@yahoo.com*

m^2/g in modified SBA-15. Finally, SBA-15 and modified SBA-15 were used as a carrier for valproic acid. The release studies were carried out at λ max = 205 nm by UV-Vis. The results indicated that the release of the drug increased with increasing pH and time. As the drug moves, the digestive tract increases from the stomach to the intestine, and a pH of 6.8 resembling the best results as compared with pH 1.2.

Keywords: Mesoporous SBA-15 nanoparticles, Valproic acid, Drug delivery, Release, Carriers.

1. Introduction

According to the name of the IUPAC, the term "porous" refers to a substance that has nano-sized cavities. The porous microstructure has a cavity diameter smaller than 2 nm, mesoporous material has a cavity diameter in the range of 2 to 50 nm, and the coarse porous material has a diameter of the cavity larger than 50 nm [1]. In cases where large molecules such as enzymes, proteins, and large hydrocarbon molecules present in crude oil are intended to perform a reaction, porous materials with small pores exhibit many limitations and deficiencies. A lot of research has been done in the synthesis of porous materials with larger pore sizes [2]. Porous solids with their unique structural composition combine to have significant potential for the development of various processes, such as environmental processes and industry [3]. These materials have important applications in the field of ion exchange, petroleum refining, petrochemicals, catalysts, adsorbents, gas separation, agriculture, etc. [4-8].

One of these porous materials is SBA-15, which consists of six-cornered silicate cavities that are arranged in parallel and very well together [9]. One of the most prominent features of SBA-15 is its extremely high-level specific surface, which in some cases amounts to 1000 m^2 / g. This mesoporous has a high thermal resistance and stables its structural order up to 550 °C [10].

Agricultural wastes, such as stems, cobs, and leaves of corn, have little economic value and are unpleasant for the environment. Today, they are part of the waste management problem. The conversion of these agricultural wastes into a silica source in the synthesis of cheap zeolites and silica can be a good way to solve environmental problems for their uses. Although silica production from agricultural wastes is not as much as in quartz or sand production, it can still be used to provide industrial needs [11,12].

In recent decades, important advances have been made in the manufacture of drugs for the treatment of various types of diseases, which has led to a better understanding of the physicochemical properties of drug molecules, as well as better recognition of cellular absorption mechanisms and, as a result, a widespread and effective therapies. Initially, chemotherapy for the treatment of diseases, common therapies, was based on the use of traditional toxic drugs that had adverse side effects and limited beneficial effects. Many of these problems are due to the absence of a clear target in anti-tumor drugs because in this case, the drug is injected into the circulatory system and involves all healthy cells and the patient. To overcome this problem, a targeted drug delivery system has been designed to carry the effective amounts of drug to target tissue cells [13]. One of the most important applications for human health care is a controlled drug delivery system. In essence, a drug delivery system can be defined as a formulation that controls the rate, time of drug delivery, drug release and targets areas of the body [14,15]. Various carriers include polymers, proteins, magnetic nanoparticles, liposomes, cyclodextrin, polyethylene glycol, and zeolites. The use of mineral carriers to control drug release is considered to be an important topic in the science of medicine and materials. There are plenty of reports about organic polymers around the drug supply [16]. However, fewer studies have been carried out on the use of mineral porous material as a carrier of medicine, and research is still ongoing [17].

SBA-15 has been considered as the potential drug carrier material according to the large surface area, big pore size, and easy surface modification [18]. Lots of interest in the physical-chemical processes has stimulated the study of silicate oligomeres in aquase alkalin solution and their possible link to zeolite nucluation and crystal groth [19]. However, laboratory and industerial synthesis involve typicaly only aquese procursor splution, several authors studying dissolved silicate oligomers have noted the effect of adding organic additives to silicate solution [20]. For example the effect of (2-hydroxyethyl) trimethylammonium (2-HETMA) cation on the equilibrium of silicate oligomers in aqueous alkaline silicate solutions was investigated using 29Si NMR spectra [21].

Some insoluble drugs like ibuprofen, nimodipine, itraconazole, have been used to control the delivery from SBA-15 [22,23]. The organic compounds can be used for modification of SBA-15 to control drug release. These compounds can modify the inner acidic [24] or basic [25] surface of channels. For example, mesoporous materials modified with amine groups and carboxylic groups were applied as carriers for the adsorption of acidic and basic drugs respectively [26,27]. Valproic acid (VPA) is one of the most important drugs used to treatment simple and complex epilepsy. In this type of epilepsy, the patient suddenly suffers from loss of consciousness, so her face remains unresponsive, remains immobile. Valproic acid helps reduce the incidence of epileptic seizures. It is also used to stabilize mood in bipolar disorder (depression-mania) and migraine, but also due to physicochemical interaction in gastric and intestinal mucosa causing a relatively high incidence of gastrointestinal complications and abdominal pain [28,29]. It has different serious side effects such as hepatotoxicity, pancreatitis, hyperammonemia encephalopathy, and coagulation disturbance. In children, the morbidity of acute pancreatitis is considered to be 2–2.7: 100,000 [30]. It was declared in the medical reports that an 11-year-old boy was accepted by the hospital with complaints of torrid tummy and diagnosed acute hemorrhagic pancreatitis. Then, SBA-15 can be a good candidate for valproic acid adsorption because of its relatively large pore size, abundant hydroxyl groups, and easily modified surface.

In this project, we intend to use the various components of the corn plant as an agricultural waste to produce the corresponding nano-silica synthesis. The objective of this project is the synthesis of SBA-15 and modified SBA-15 nanoparticles from silica corn, and the investigation of its potential in drug delivery as a carrier agent for valproic acid as well as the factors affecting the loading and releasing of drugs.

2. Experimental

2.1. Materials

The corn stems, leaves, and cobs were collected from a field around Mashhad, (IRAN). NaOH, HCl, and H_3PO_4 were also purchased from Merck. Copolymer p123 EO20PO70EO20 (M_{av} = 5800) was purchased from Aldrich. Valproic acid was obtained from Sajad Daru pharmaceutical co. Sodium dihydrogen phosphate and hexadecyltrimethylammonium bromide (CTAB), all analytical grade, were obtained from Sigma and disodium hydrogen phosphate from Merck (Germany).

2.2. Apparatus

The X-ray diffraction pattern of the silica extracted from corn waste ashes and calcined mesoporous silica was conducted by an X-ray diffractometer (Unisantis XMD300) using Cu Kα radiation at 40 kV and 30 mA. The chemical composition of silica gel in the form of powder extracted from corn ash was analyzed by X-ray fluorescence spectrometry (XRF; 8410 Rh 60 kV).

To indicate the morphology of calcined mesoporous silica, SEM images were recorded using a field-emission SEM (FE-SEM, MIRA3TESCAN-XMU). Energy dispersive spectroscopy (EDS) spectra were studied by an EDAX Genesis XM2 attached to FE-SEM.

In this work, transmission electron microscopy (TEM, JEOL 2100, 200 kV) was used to study the pore structure of the materials.

On an FT-IR spectrophotometer (Bruker-Vector 22), in the range of 500–3500 cm−1 using KBr pellet, the vibrations and FT-IR spectra of mesoporous silica were recorded.

The specific surface areas of the samples were determined with the Brumauer–Emmett–Teller (BET, model BELSORP mini 100 instruments). The pore size (diameter DBET) distribution was calculated from nitrogen adsorption data using the conventional Barrett–Joyner–Halenda (BJH) method. TGA (Netzsch STA 409) was used to evaluate the thermal characteristic of mesoporous silica.

For the determination of drug concentration, UV-Vis absorbance spectra were recorded using a Cecil CE5501 spectrophotometer (Hach dr 5000).

The value of pH was determined by SevenEasy pH Mettler Toledo AG, Switzerland.

2.3. Extraction of silica from corn ash

For extraction of silica, the corn stems, leaves, and cobs were collected from a field around Mashhad, (IRAN) and washed with water to remove soil and contaminants. The stems, leaves, and wood were dried at 100 °C and separately burned to ashes in the open air. In order to remove the disturbances and obtain pure silica, the ashes of each part were separately immersed in a 1 molar HCL solution for 4 hours, then the acidic solution was filtered, and washed with distilled water several times to neutralize.

After acid washing, each of the three parts, stems, leaves, and corn of the corn separately dried in an oven at 100 °C over-night and placed in a furnace at 600 °C for 24 hours until all the organic matter exposed in the ash of the stems, leaves, and wood of the corn plant. Further, 10 g of each ash was heated with 60 ml of 1 M NaOH, and then the resulting mixture was filtered. The residue was heated to 60 ml with distilled water and the resulting mixture was refined. The fluid was added from the two previous steps. After cooling the liquid, the solution was neutralized by one molar HCl to form a gel. Once the gel has been formed, it gives one day to complete the formation of the gel. The resulting gel was then washed with distilled water and placed in an oven at 80 °C for 12 hours [30]. The silica obtained in the mortar turned into powder and was prepared for analysis.

To investigate the effect of final silica washing after extraction, the silica obtained from the previous step was again washed with distilled water and separated by centrifugation.

Extraction of silica from corn plants is shown in Fig. 1.

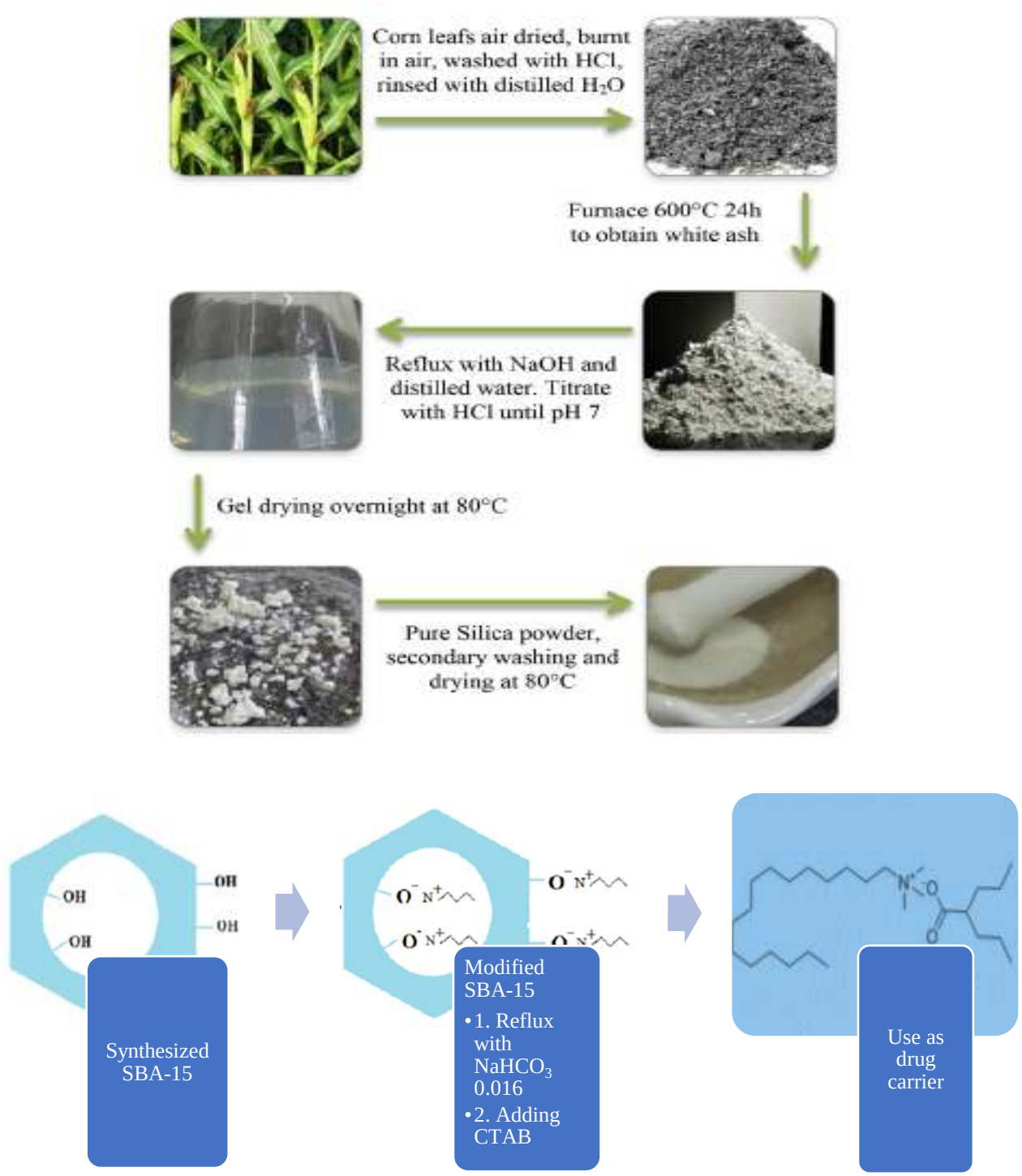

Fig. 1. Schematic of extraction of silica from corn and synthesized modified SBA-15.

2.4. Synthesis of mesoporous SBA-15 nanoparticles

Silicate solution was prepared according to Kalapathy et al. [31], approach with some changes. An appropriate quantity of silica extracted of corn (2.67 g) dissolved in 2 M NaOH (Merck, 98%,) solution at 50 ◦C for 6 h and used as a silica source for the synthesis of mesoporous SBA- 15 nanoparticles.

SBA-15 was synthesized using silica powder extracted from corn ash according to Azizi et al [32]. At first, copolymer p123 (3 g) was dissolved in an acidic solution of 85 wt % H_3PO_4 (3.61 g of in 55 ml of distilled water) under stirring in an oil bath at 40 ◦C until a clear solution was obtained. Alkaline sodium silicate solution was quickly added to this mixture.

H_3PO_4 (1.84 g) was dissolved in 5 ml water and added to the above solution and excess water was added until the volume of solution was reached 80 ml. 2 min after the addition of H_2O to solution, stirring was stopped. Then, synthesized gel was transferred to a polypropylene bottle and heated at the same temperature in an oil bath under stirring for 48 h. Then put in the autoclave for 24 h at 100 ◦C. The resulted products were filtered, washed with distilled water, and dried in an oven at 70 ◦C. Subsequently, the sample was calcined at 550 ◦C for 7 h to remove the organic template. Synthesized SBA-15 nanoparticles in the form of white powder were obtained and were stored for further applications.

2.5. Modification of SBA-15

Modification of nano-adsorbent was included in the following processor. At first, the amount of 0.1 g of SBA-15 absorber and 25 ml of $NaHCO_3$ 0.016 was deposited in the balloon and placed on a heater for 2 hours in a paraffin bath. The temperature was fixed at 100 °C and the mixture of SBA-15 and $NaHCO_3$ was refluxed for 24 hours, then the extra NaHCO3 solution was separated. The next step was the stabilization of the $CTAB^{-}O$ cationic surfactant, in which the OH group is bound to SBA-15 to ÅO-SBA, adding 3 ml of CTAB (20,000 mgL^{-1}) and after 24 hours at 50 °C, reflux, then transfer the contents of the balloon to a human body and place the human in an oven at 50 °C to dry [33]. The modified SBA-15 Mechanism is shown in Fig. 1.

2.6. Drug loading

10.0 g of synthesized SBA-15 were soaked with 500 ml of water solution of 15 mg/ml valproic acid. The adsorption process was performed at room temperature for 24 h. The concentration of valproaic acid was determined by a UV-Vis spectrophotometer [34] at 205 nm. The amount of drug adsorbed on to modified SBA-15, q_t (μg/g), at time t was calculated using below Equation:

$q= (C_0-C_T)V/M$

where C_0 (mgL^{-1}) is the initial adsorbate concentration, V(L) is the volume of the drug solution in the flask, C_T (mg/L) is the drug concentration after time t and M (g) is the mass of dry adsorbent [35,36]. After adsorption, the sample was filtered and dried at room temperature for 24 h and another 24 h at 100 °C, for the release study.

2.6. In-vitro drug release

The release of valproic acid from powdered samples was performed in two buffered solutions with different pH 1.2 (stomach), 6.8 (intestine), at 37 °C with a stirring rate of 250 rpm. Phosphate buffer solution (PBS) was prepared by mixing sodium hydrogen phosphate (0.1 M) and disodium hydrogen phosphate (0.1 M) solutions. 200 mg of drug-loaded nanoparticle SBA-15 was added into 20 mL of each buffered solution. After the indicated period of times (0.30–24 h) the sample of the drug (alternatively suspension) was centrifuged for 15 min and supernatants separated for drug determination.

The concentrations of released drugs were measured by UV-Vis spectrophotometer at 205 nm.

3. Result and discussion

3.1. Composition of corn and characterization of nano silica and synthesized mesoporous SBA-15 nanoparticles

XRF analysis was used to determine the amount of silica in different parts of stem, leaf, and corn cob. The results of this analysis are presented in the following tables. According to Table 1, the highest percentage of the oxides present in the plant was related to the silica (SiO_2) in the leaves with 93.53% in comparison with 83.30% in the stems and 21.1% in corn cobs. Regarding the fact that in this study on the corn plant, a high percentage of silica was found in the leaves, then pure silica was synthesized from the leaves.

Table 1. Chemical compositions of different parts of corn ash (wt%) by XRF. LOI, loss of ignition.

parts	SiO_2	Al_2O_3	Na_2O	MgO	K_2O	TiO_2	MnO	CaO	P_2O_5	Fe_2O_3	SO_3	LOI
Stem	83.30	2.22.	0.88	2.65	3.20	0.19	0.09	1.94	2.92	1.47	0.16	0.74
Leaf	93.75	0.83	1.87	1.87	1.63	0.10	0.04	0.60	0.24	0.750	0.10	0.17
Cob	21.10	0.95	2.43	12.15	3.18	0.59	0.12	14.31	19.14	5.19	0.6	20.06

The XRD pattern obtained from the silica extracted from the leaf ash is shown in Fig. 2. a. This specimen has a broad-spectral width in the region 2θ=22, which indicates the amorphous and formidable silica produced. This is important for the synthesis of zeolites and mesoporous material because this broad peak shows the formation of amorphous silica. Therefore, according to the form of amorphous silica, it can be used in the synthesis of mesoporous and zeolites.

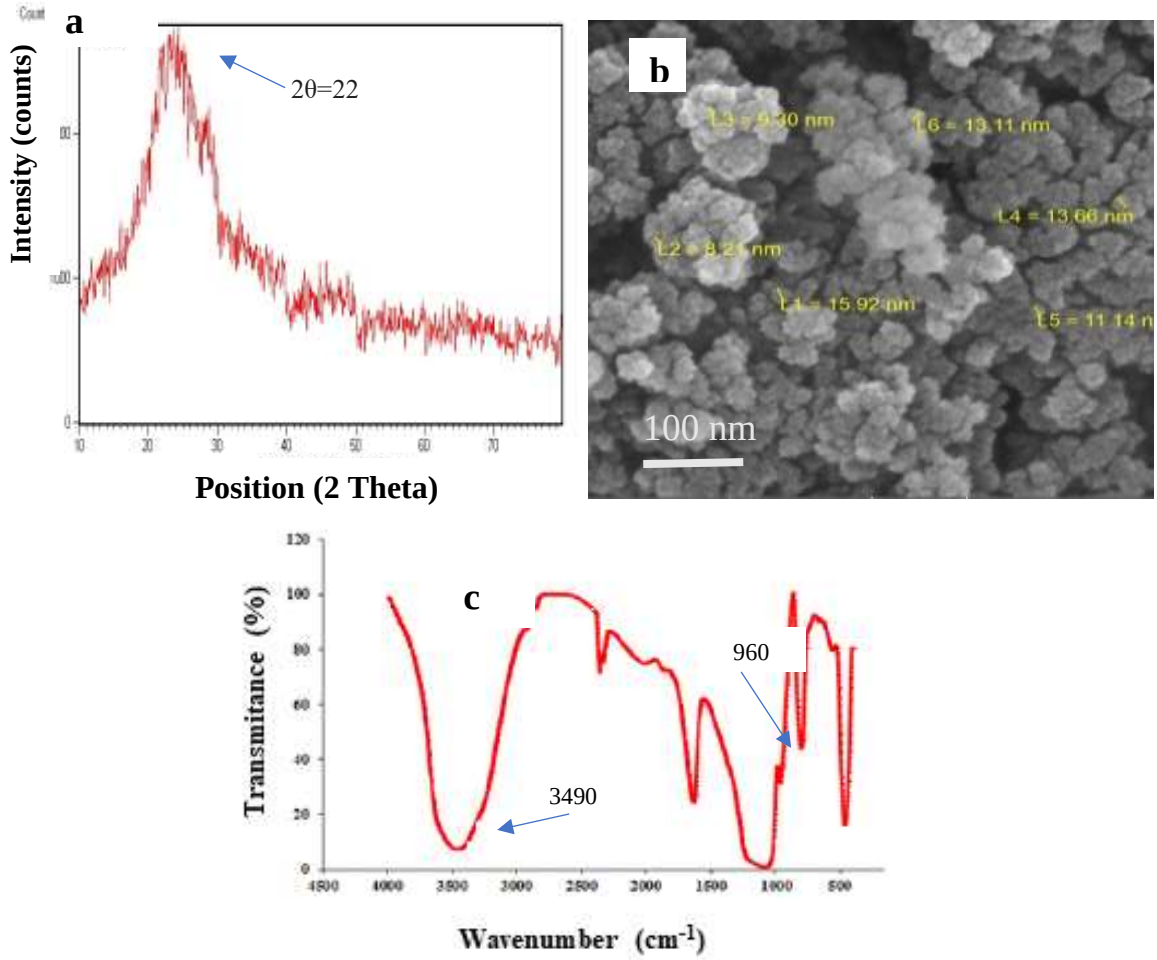

Fig. 2. a) XRD pattern from silica corn; b) SEM image of silica nanoparticles; c) FT-IR spectrum of silica nanoparticles.

To illustrate the shape and the size distribution of the synthesized silica particles, the SEM images were studied. Fig. 2.b shows the SEM images obtained from the sample of silica nanoparticles (100 nm). The sample consists of a mixture of spherical and uniform particles that have an average diameter of 8 to 15 nm.

The important chemical groups in the silica extracted from the corn leaf are determined using the FT-IR spectrum, as shown in Fig. 2. c. The narrow strips in the range of 500 cm^{-1} and 800 cm are related to various oscillating modes of Si-O or O-Si-O in the silica network. The dominant peak in the region of 1000 cm^{-}

[1] to 1300 cm^{-1} is due to siloxane (Si-O-Si) bonds, and the band within the range of 960 cm^{-1} is related to the tensile fluctuations of the silanol groups. The strong peak at near, 3500 cm^{-1} is related to the hydroxyl group of the silica.

In the case of SBA-15, a low angle x-ray diffraction method was used to investigate and determine the special structure of nanoparticles of mesoporous silica. An XRD pattern typical of SBA-15 is shown in Fig. 3. a. The presence of a significant peak in relation to the diffraction from the 2 Theta or in miller index (100) indicates the formation of the hexagonal ordered structure of SBA-15 [37]. Smaller peaks at the higher diffraction angles of the plates (110) and (200) also represent the structural order of the SBA-15. Also in Fig. 3. The XRD pattern of the SBA-15-drug is shown, and it can be seen that there are no diffrences in peaks. It shows that the structure of mesoporous material doesn't change after loading the drug.

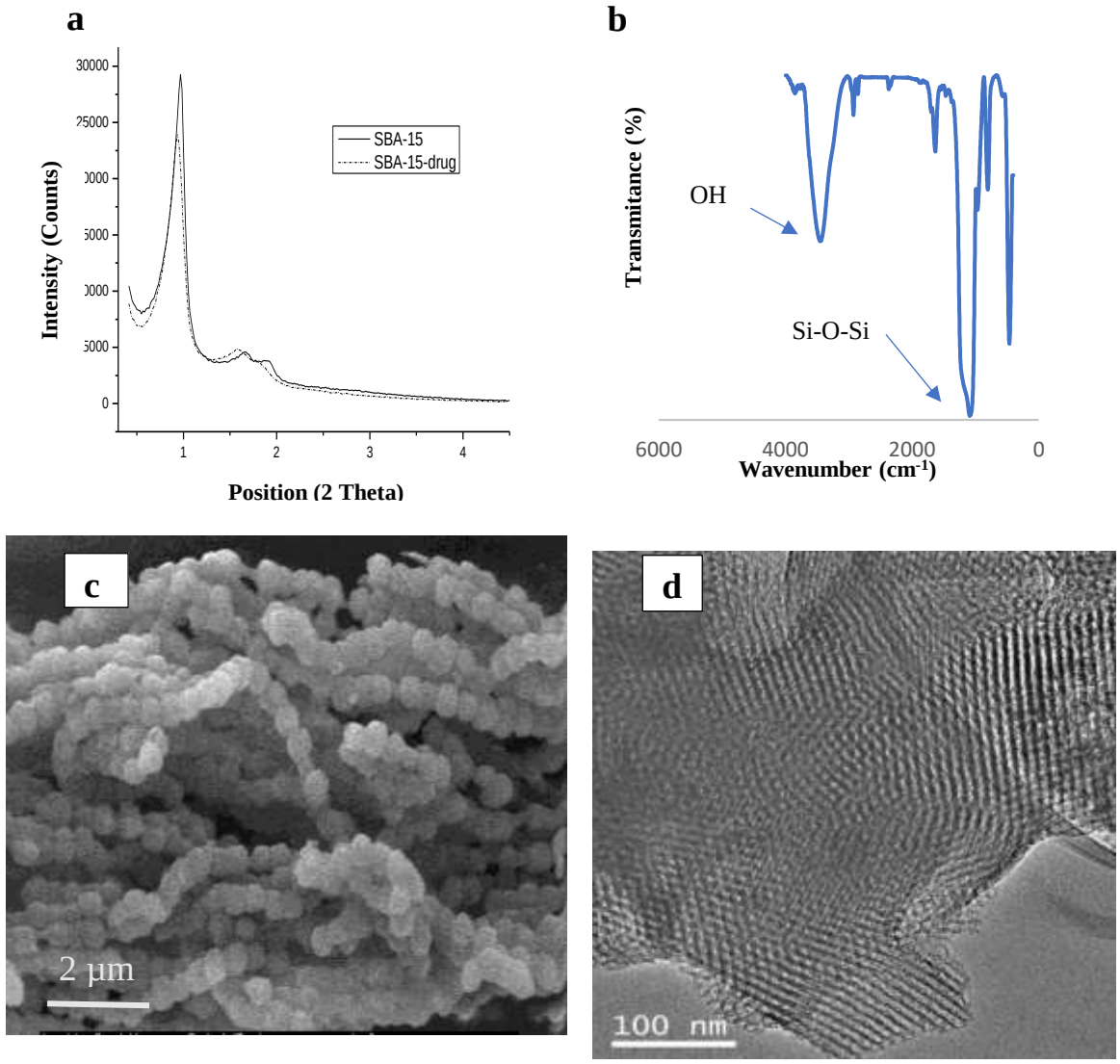

Fig. 3. a) XRD pattern typical of SBA-15 and SBA-15-drug; b) FT-IR spectrum of SBA-15; c) SEM image of SBA-15; d) TEM image of SBA-15.

The infrared spectrum of the nanoparticles of the synthesized mesoporous in the range of 500-4000 cm^{-1} was shown in Fig. 3. b. In the infrared spectrum of nanoparticles, the mesoporous silica particles exhibit a strong and wide absorption peak in 773 cm^{-1} related to Si-C tensile vibrations. Symmetric vibrational states contain two main components, namely, the movement of the two-atomic oxygen atom adjacent to the central

silicon atom and the outward-phase motion of two oxygen atoms with respect to the central atoms [38]. In addition, each symmetrical vibrational state is associated with optical transverse optical and optical path length. The two absorption bands in 1235 and 1039 cm^{-1} related to the transverse optical stretching and Si-O-Si optical length, respectively. A strong and wide absorption band is attributed to asymmetric stretching vibrations in the region 1000-1300 cm^{-1} [39]. In 1138 and 1183 cm^{-1}, when the pairs of non-symmetrical, longitudinal, and transverse optical strips overlap [40], they create a large absorption band in the area of 1,000-1,300 cm^{-1}. The peak 3417 corresponds to the hydroxyl group and the stretching vibrations of the silanol group [41]. The absorption band in 960 does not react to the overlap of SiO_2 vibration modes, and the tensile vibrations of silanol are attributed [42]. The strong peak at near, 3500 cm^{-1} is related to the hydroxyl group of the silica. The absorption bar at 550 cm^{-1} indicates the formation of the SBA-15 cavity wall [43].

Isolated small hexagons are observed in Fig. 3. c as SEM images. Transmission electron microscopy (TEM) involves the use of a high voltage electron beam which is emitted by the cathode and formed with the help of magnetic lenses. The electron beam which is transmitted from the specimen carries information about the structure of the specimen. The spatial variation in the image is magnified with a series of magnetic lenses before it hits the detector. The images produced by this type of electron microscopy are two-dimensional in nature. Fig. 3. d shows a TEM image of SBA-15 and the pore can be seen in the image with bright and dark contrast. Bright regions mark the pores, with the dark regions making the pore walls of mesoporous silica. Also, it is possible to see the channels in the TEM image.

Using some physical absorption of nitrogen, some physical properties of porous silica nanoparticles were investigated. The synthesized nanoparticle absorption component is shown in Fig. 4. According to the IUPAC classification, this homogeneity is related to the mesoporous material, indicating that the pore size of the sample is located within the mesoporous range. This homogeneity has a waste loop in the region 0.6-0.9 (p/p_0) which may indicate a change in mesoporous tissue. Also, this waste cycle may indicate a significant additional amount of mesoporous. This is confirmed by the BJH design, which shows the size distribution of the cavities. This shape clearly shows the distribution of the two peaks of mesoporous, which can be due to the formation of these two peaks of mesoporous, for the following reasons: 1- Interference between surfactant and SiO_2. 2- Hydrolysis of SiO_2 to Surfactant. 3- Adjust pH reaction. 4- Relative Hydrolysis Rate of SiO_2. 5- Condensation due to pH setting. Table 2 shows that modifying SBA-15 can decrease the surface area of nanoparticles of SBA-15 because surfaces are occupied with the surfactant.

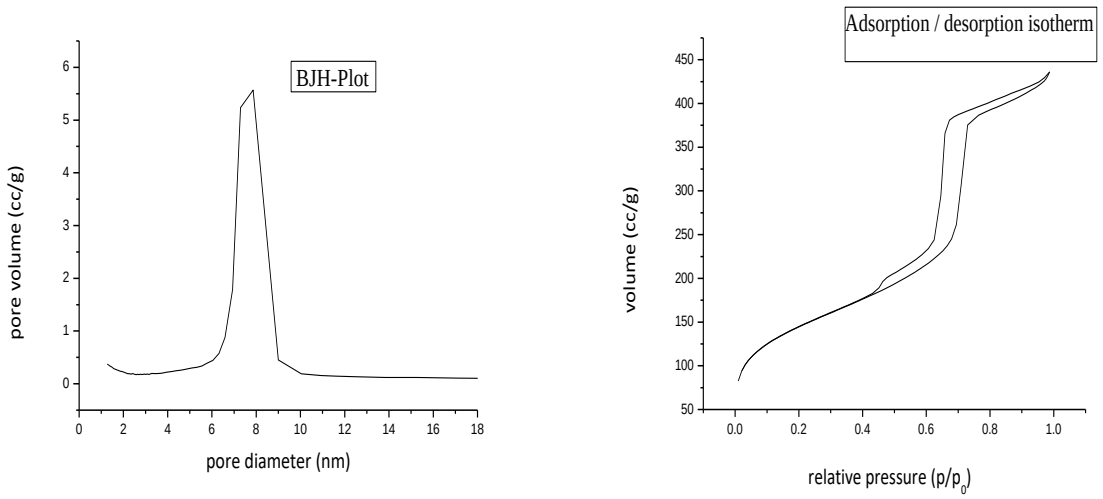

Fig. 4. BET & BJH of SBA-15.

Table 2. BET analysis of SBA-15 & modified SBA-15

	BET Surface area (m^2/g)	BET total pore volume (cm^3/g)	Mean pore diameter (nm)
SBA-15	488	0.67	7.5
Modified SBA-15	127.7	0.49	5.5

The TGA profile of SBA-15 has a major peak of weight loss in the range of 150-250 °C, assigned to the loss of surfactant by mesoporous, the thermal decomposition of surfactant (Fig. 5). The weight loss of 5 % at around 180˚C < in the first step is due to the existent water in the nanocomposites. At T>180 ˚C, a continuous and big weight loss is observed, which could be related to the combustion of organic material. Physical removal of absorbed water molecules is observed at 90 °C. According the table. 3 in modified SBA-15 there are more organic materials than it is modifier. Then, the percentage of weight loss in the range of 180 ˚C and 900 ˚C is increased, and it can be understood that all the pores are filled with CTAB because after modification of SBA-15 the total percentage of weight loss is 30% that it is near to 13% in SBA-15.

Table 3. The weight loss of SBA-15 & modified SBA-15

Sample	T < 180˚C	180˚C < T < 900 ˚C	Total
SBA-15	5 %	8 %	13 %
Modified SBA-15	10 %	20 %	30 %

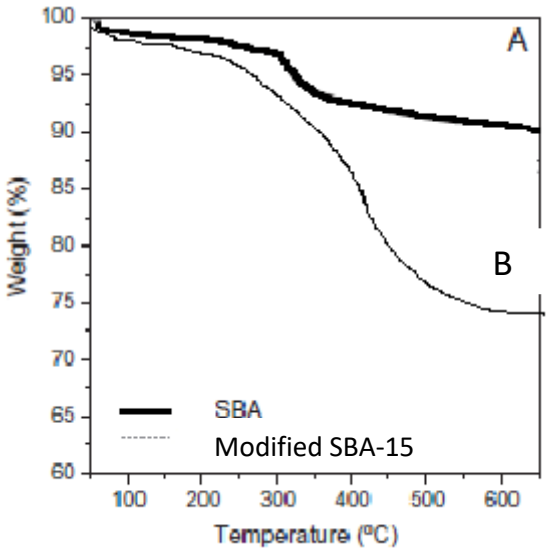

Fig. 5. TGA profile of A: SBA-15, B: Modified SBA-15

To illustrate the size, shape, and distribution of mesoporous silica nanoparticles, a scanning electron microscope was used. Fig. 3. c shows the obtained SEM images of the sample SBA-15 that is formed by spongy agglomerated nanoparticles, revealing the growth of hexagonal-shaped domains. However, in Fig. 6. The SEM image shows that after drug loading the more vacant spaces are filled with drugs. Fig. 6. b shows after modification, the particle of CTAB were attached on the surface and within the pores of the SBA-15 in comparison with SBA-15, confirming the findings observed by BET.

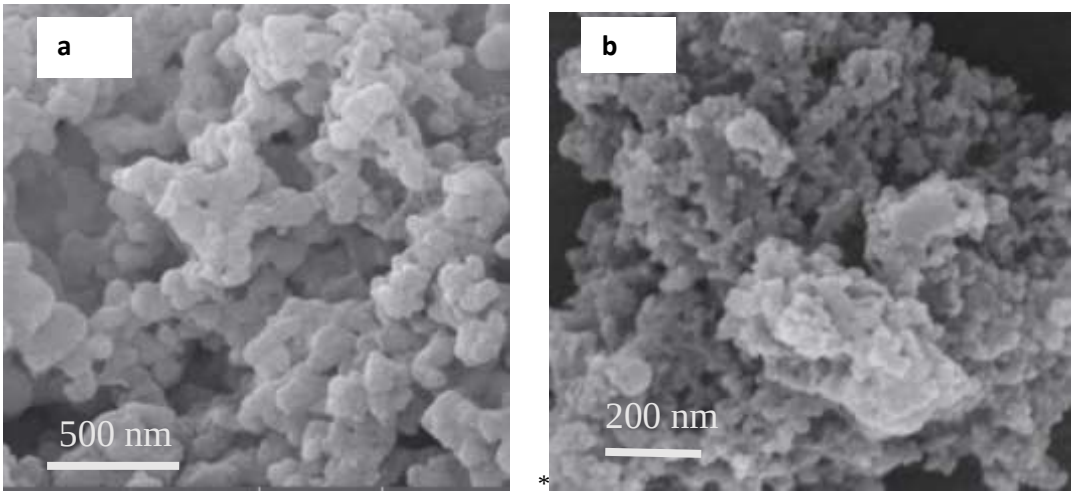

Fig. 6. a) SEM images of SBA-15 after drug loading; b) SEM image of modified SBA-15 with CTAB

3.2. Adsorption and Drug release studies

Valproic acid is an anionic drug and should easily interact with a positive group, and bonds production is stronger than simple physical absorption on SBA-15 silanol groups. Table 4 shows the basic information about the interactions of valproic acid with both modified and unmodified SBA-15. The results show that the concentration of surfactant is higher, the better absorption of valproic acid. The molar ratio between valproic acid and CTAB shows that interaction with valproic acid is best in relatively low CTAB groups. This is because the better availability (for medicine) of the functional groups is rarely distributed. For content above functional groups, all available sites for absorption are not used due to the effects of the steric barrier caused by the size of the drug molecule [44]. In comparison, drug accumulation posed a lower risk as VPA is not the primary substrate for the majority of drug transporters across the placenta and lastly [45].

All the suggested mechanisms (and possibly many more) may be contributing factors, together with inter-patient variability, environmental and lifestyle factors, each of which is also undefined, and lead to an increased risk of the teratogenic effects of VPA [45].

Table 4. Adsorption of valproic acid on SBA-15 & modified SBA-15.

Sample	q_t (μg/g) [a]	Amount of CTAB (gr)
SBA-15	89.10	-
Modified SBA-15	95.22	0.03
Modified SBA-15	106.92	0.06
Modified SBA-15	93.32	0.09

a: Amount of adsorbed on to SBA-15 & modified SBA-15.

Results show the release of the drug increases with pH. Therefore, a drug increases its release by moving down the gastrointestinal tract from the stomach to the intestines.

To investigate the potential of using SBA-15 and modified SBA-15 as a drug carrier, the drug release rate in 2 buffer solutions at pH of 1.2, 6.8 at 37 °C was measured and plotted in Fig. 7. The results showed that with increasing pH, the drug in the gastrointestinal tract moves from the stomach to the intestine and causes it to be more released in the intestine. Therefore, it can be concluded that with this carrier, some side effects of the drug can be avoided. The amount of drug loading and release has increased by about 20%. Therefore, it can be said that modifying the SBA-15 can help absorb more drugs.

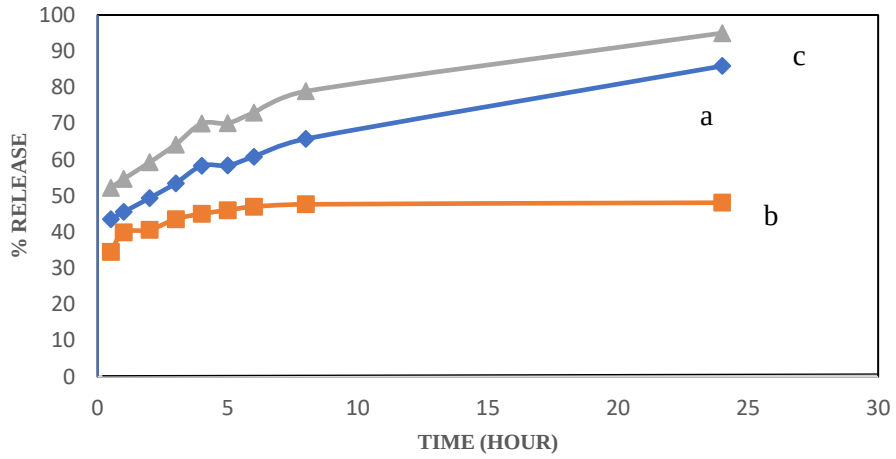

Fig. 7. Cumulative release profiles of valproic acid from SBA-15 (a: 6.8, b: 1.2) and modified SBA-15 (c: 6.8) in different pH.

3.3. First pseudo-kinetic pattern

In 1898, the Lager Gren showed the first-order equation for absorbing the absorbent material from aqueous solution on coal [46]. This initial equation was based on the kinetic equation for absorbing total/liquid systems based on gravity capacity in the adsorption phenomenon, which is widely used to describe how adsorption kinetics are used. This model assumes that the rate of change in absorption of the sample with time is directly proportional to the difference in saturation concentration of the adsorbed molecule on the adsorbent surface and the amount of absorption with time. The first-order Lagrange acceleration equation is called the first-order company equation [47]. This equation is as follows.

$$dq_t/dt = K_1 - (q_e - q_t)$$

In this equation, q_e and q_t, respectively, is the adsorbed material on the carrier at the time of equilibrium t in mg/g and K_1, is the pseudo-first-rate constant in terms of (h^{-1}).

By integrating the equation and applying the conditions t = 0 to t = t and $q_t = 0$ to $q_t = q_t$, the form of the equation is converted as follows.

$$\text{Log } (q_e - q_t) = \log q_e - \frac{k1}{2.303} t$$

The graph in times of t is linear and the values of k_1 and q_e, k_1 are obtained from the origin and gradient.

The log (q_e-q_t) graph in terms of t is shown in Fig. 8 for the first-order kinetics at different initial concentrations of the drug and therefore the diffusion process is the rate of absorption process because if the experimental data are in accordance with the first-order kinetic model, the propagation process is the absorption rate controller [48-50].

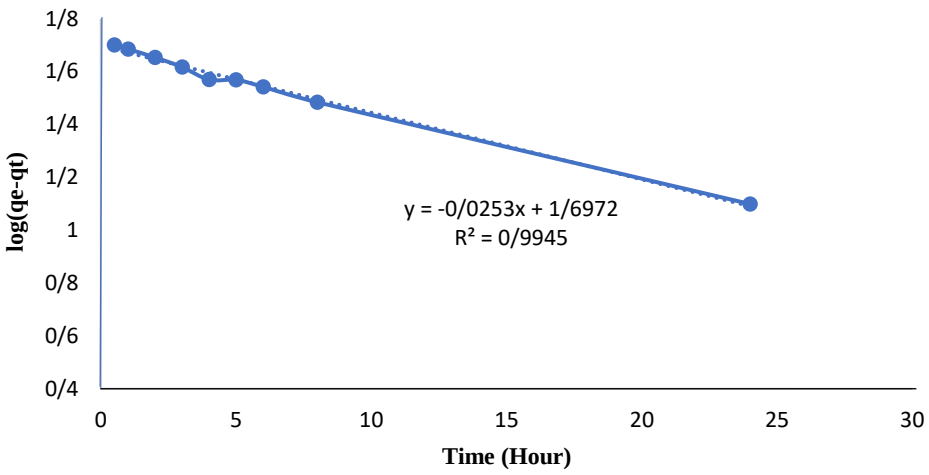

Fig. 8. The first-order kinetic of drug absorption by SBA-15.

4. Conclusion

Our studies have shown that the corn plant is a very suitable and economical resource for the extraction of silica and the preparation of SBA-15 nanoparticles. These methods that used in this study are fast and easy. The preparation of these nanoparticles was carried out in simulated human conditions. The study on SBA-15 showed that these nanoparticles could be suitable for pharmaceutical carrier applications. This study investigates the absorption and release of the valproic acid drugs on the SBA-15 nanoparticle as a carrier of the drug. The absorption of valproic acid on the surface of the desired nanoparticles was very successful. This drug carrier can reduce toxicity and increase the effectiveness of the drug and also control the amount of drug release in the body.

Refrences

[1] S. John. P, A Guide to materials characterization and chemical analysis. WILEY-VCH: NewYork., (1996).

[2] T. Akira, S. Ferdi, *Microporous Mesoporous Mater*. **77** (2005) 1.

[3] M. Lynne, L. Friedrich, E. George, *in Pure and Applied Chemistry*, **73** (2001) 381.

[4] W. Hölderich, J. Weitkamp, H. G. Karge, H. Pfeifer, W. Hölderich, Zeolites and Related Microporous Materials: State of the Art, **84** (1994) 1375.

[5] B. Donald W. *Zeolite Molecular Sieves: Structure, Chemistry, and U*se. John Wiley & Sons New York. 1974.

[6] S. Mohammad, R. Ali, A. Mehdi, M. Ali. *Advanced Powder Technology*. **30** (2019) 1823.

[7] Kh. Faezeh, R. Bibi marziyeh, A. Seyed Naser, *Journal of Applied Chemistry*, **16** (2021) 165, in Persian.

[8] M. Ali, R. Mohammad, A. Masoumeh *ChemistrySelect*. **2** (2017), 4439.

[9] Q. Wei., H. Q. Chen., Z. R. Nie., Y. L. Hao., Y. L. Wang., Q. Y. Li., J. X. Zou., *Mater. Lett*, **61** (2007) 1469.

[10] M. Randy, R. Maarten B. J, H. Kristof, V S. Michiel, D, Gert, A. G. J. Jasper, M. Guy, A. Patrick, H. Johan and A. M. Johan, *Phys Chem Chem Phys*, **13** (2011) 2706.

[11] F. C, A. Chik, B. Md, *Advanced Materials Research*, **626** (2013) 997.

[13]S. Igor, V. John, W. hia-Wen, L. Victor, *J. Am. Chem. Soc*, **60** (2008) 1278.

[14] Y, Jin-Wook, L. Chi H, *J. Controlled Releas*, **112** (2006) 1.

[15] T. Vladimir, Nature reviews. *Drug discover*, **4** (2005) 145.

[16] P. Haesun,P. Kinam, *Pharm. Res*, **13** (1996) 1770.

[17] H. Patricia, S. Christian, M. Guillaume, R. Naseem, B. Francisco, V. María, S. Muriel, T. Francis, and F. Gérard, *Solid State Sci*, **8** (2006) 1459.

[18] Z. Dongyuan, F. Jianglin, H. Qisheng, M. Nicholas, H. F, Glenn, F. C. Braley, D. S. Gallen, S*cience*, **279** (1998) 548.

[19] S. Abdolraouf, G. Nasser, *Spectrochimica Acta Part A* , **65** (2006), 753.

[20] S. Abdolraouf, G. Nasser, B. Hamidreza, *Journal of solution chemistry*, **34** (2005), 283.

[21] G. Nasser, G. Mohammad, Ch. Arab, B. G, *Journal of Molecular Structure*, **930** (2009), 2.

[22] Z. Dongyuan, H. Qisheng, F. Jianglin, F. C. Bradley, and D. S. Galen, *J. Am. Chem. Soc*, **120** (1998) 6024.

[23] Y. Hui, Z. Qing-Zhou, *Microporous Mesoporous Mater*, **123** (2009) 298.

[24] I. K. Rukhsan, A. Irshad, P. Kavita, Kh. N.H, A. Sayed H.R. V.Jasra. R, *Catal. Commun*, **10** (2009) 572.

[25] L. Zhaohua, F. Jay A, W. Jan B, E.M. Donald, *Microporous Mesoporous Mater*, **83** (2005) 150.

[26] Z. Wei, Q. Xuefeng, Y. Jie, Z. Zikang, *Mater. Chem. Phys*, **97** (2006) 437.

[27] T. Qunli, X. Yao, W. Dong, S. Yuhan, *J. Solid State Chem*, **179** (2006) 1513.

[28] G. Liliana, M. P. Juan Carlos, *J. Chem*, (2013) 1.

[29] L. Tesy, B. E, M. O. Luisa, M. J, A. Roberto, *Optical Materials*, **29** (2006) 75.

[30] L. Van Hai, T. Chi Nhan Ha and T. Huy Ha, *anoscale Res Lett*, **8** (2013) 58.

[31] K. Uruthira, *Bioresour. Technol*. **73** (2000) 257.

[32] A. Seyed Naser, Gh. Shahram and Ch. Elham, *Electrochimica Acta*, **88** (2013) 463.

[33] M. Ali, Sh. Shila, *Journal of Applied Chemistry* (JAC), 9 (2016) 11, in Persian.

[34] K. Danina, D. Aleksandra, M. Maja, M. Anđelija, K. Marco, B. DB, et al. *Colloids and surfaces B, Biointerfaces*, **1** (2011) 65.

[35] J. Bhakta, Y. Munekage. *Int. J. Environ. Res*, **5** (2011) 585.

[36] H. B, K. R, S. S, *J. Hazard. Mater*, **162** (2009) 305.

[37] I. Pilinio, *J. Non-Cryst. Solids*, **316** (2003) 309.

[38] K. C. T, Eur. *Phys. J. B*, **38** (1988) 1255.

[39] G. Frank, *Phys. Rev. B*, **19** (1979) 4292.

[40] W. Jianping, Z. Bingsuo, AEI. Mostafa, *J. Mol. Struct*, **508** (1999) 87.

[41] P. N, V. C and L. Michel, *Thin Solid Films*, **310** (1997) 47.

[42] A. Rui M and P. Carlo G, Structural Investigation of Silica Gel Films by Infrared Spectroscopy, **68** (1990) 4225.

[43] C. Gisèle, N. Claude and V. Jacques, *J. Chem. Soc., Chem. Commun*, (1982) 1413.

[44] M. Michal, L. Marek, *J. Solid State Chem*, **184** (2011) 1761.

[45] L. Katie Alexandra, *Bioscience Horizons : The International Journal of Student Research*, **6** (2013).

[46] L. Svenska, *Kungliga Svenska Vetenskapsakademiens Handlingar*, **24** (1898) 1.

[47] H. Yuh-Shan, *Scientometrics*, **59** (2004) 171.

[48] A. Saeid, *J. Colloid Interface Sci*, **276** (2004) 47.

[49] R. Ali, B. Samaneh, M. Soheil, R. Nadia, M. Ali. *Heteroatom Chemistry*, **28** (2017), 21396.

[50] S. Amir, M. Ali, *Progress in Reaction Kinetics and Mechanism*, **40** (2015) 383.